

Are your **MRI contrast agents** cost-effective?

Learn more about generic **Gadolinium-Based Contrast Agents**.



FRESENIUS
KABI

caring for life

AJNR

Predicting Brain Tumor Histology: Change of Effective Atomic Number with Contrast Enhancement

Richard E. Latchaw, J. Thomas Payne and Ruth B. Loewenson

AJNR Am J Neuroradiol 1980, 1 (4) 289-294

<http://www.ajnr.org/content/1/4/289>

This information is current as of April 18, 2024.

Predicting Brain Tumor Histology: Change of Effective Atomic Number with Contrast Enhancement

Richard E. Latchaw¹
J. Thomas Payne^{1, 2}
Ruth B. Loewenson³

Thirty-eight enhancing intracranial neoplasms were evaluated with a dual kilovoltage technique to measure the change of effective atomic number (ΔZ), and linear attenuation coefficients with the use of iodinated contrast material. The change of effective atomic number was found to separate intracranial neoplasms into three major groups: gliomas, meningiomas, and metastases. Other parameters, including linear attenuation coefficients and CT numbers, varied from less accurate to inaccurate. The change of effective atomic number with contrast enhancement not only predicted the appropriate histologic group of the neoplasm, but also aided in the differential diagnosis of neoplasms without a characteristic ΔZ value.

We have described a sensitive method for histologically grouping intracranial neoplasms preoperatively using computed tomography (CT) [1]. The effective atomic number and change of that number with contrast enhancement was found for each of 15 tumors using two different kilovoltage settings during CT. These values were correlated with the pathologically determined histology. This technique allowed the neoplasms to be effectively separated into three histologic groups: gliomas, meningiomas, and metastases with a high degree of statistical significance. Although the initial series of cases was small, this did not detract from the statistical significance, however, a larger experience was necessary to test the efficacy of the method in a greater variety of neoplasms. We describe this additional experience.

Received November 28, 1979; accepted after revision April 7, 1980.

Presented at the annual meeting of the American Society of Neuroradiology, New Orleans, Louisiana, February 1978.

¹Department of Radiology, Box 292 Mayo Memorial Building, University of Minnesota Hospitals, Minneapolis, MN 55455. Address reprint requests to R. E. Latchaw.

²Present address: Department of Radiology, Abbott-Northwestern Hospital, Minneapolis, MN.

³Department of Neurology-Biometry, University of Minnesota, Minneapolis, MN 55455.

This article appears in July/August 1980 *AJNR* and October 1980 *AJR*.

AJNR 1:289-294, July/August 1980
0195-6108/80/0104-0289 \$00.00
© American Roentgen Ray Society

Materials and Methods

Case Material

There were 38 intracranial neoplasms evaluated in 37 patients: one patient had two metastatic lesions. Of the lesions, 15 were described previously [1], and 23 new cases have been added. The histology of each is listed in table 1. There were 14 gliomas, seven meningiomas, and five metastases. In addition, there were six neurinomas, primarily acoustic; three histiocytic lymphomas; two pituitary tumors; and one pinealoma. Two neuropathologists reviewed all pathologic material for histologic diagnosis, including grading of degree of malignancy.

All tumors had increased attenuation coefficients relative to the normal brain either before or after contrast enhancement, and had varying degrees of enhancement. No neoplasm had lesser attenuation than the normal brain. Contrast enhancement was accomplished in all cases with a 50 ml bolus of meglumine diatrizoate (14 g iodine) (Hypaque 60, Winthrop Labs.), followed by a 300 ml infusion of Reno-M-DIP (42 g iodine, Squibb) given over 4-5 min. Children received lesser amounts, not more than 3 ml of 60% contrast/kg.

TABLE 1: Intracranial Neoplasms Case Material

Pathology/Case No.	%ΔZ	μ spread	%Δ ^μ 90
Astrocytoma:			
Grade 1:			
1	7.1	23.0	0.5
Grade 1-2:			
2	6.2	0.0	2.3
3	9.9	17.1	3.8
Grade 2-3:			
4	18.4	41.0	3.9
Grade 3:			
5	7.2	11.0	1.4
Grade 4:			
6	7.4	13.0	1.4
7	2.8	1.7	1.0
8	7.0	11.7	3.3
9	7.0	16.6	2.3
10	17.1	36.0	2.9
Brainstem astrocytoma:			
Grade 2:			
11	17.8	41.6	6.6
Grade 1:			
12	0.0	0.0	0.5
Medulloblastoma:			
13	8.7	18.0	2.8
14	16.4	32.0	3.8
Meningioma:			
15	15.0	30.0	2.4
16	17.0	32.0	2.6
17	17.0	43.0	6.9
18	12.0	29.0	3.5
19	17.1	36.3	5.2
20	17.1	38.0	4.8
21	13.9	25.0	1.9
Pituitary adenoma:			
22	15.0	33.0	3.0
23	9.9	20.0	1.5
Neurinoma:			
Trigeminal:			
24	6.8	7.7	3.3
Acoustic:			
25	23.9	41.6	3.8
26	20.0	33.0	4.2
27	58.0	167.0	12.0
28	42.0	100.0	10.5
29	24.7	58.0	4.8
Pinealoma (germinoma):			
30	3.7	7.0	2.4
Histiocytic lymphoma:			
31	15.0	34.0	3.8
32	13.6	52.0	5.2
33	26.0	58.3	4.7
Metastasis			
Prostate:			
34	24.0	48.0	3.8
Lung:			
35	29.0	68.0	4.2
36	18.0	34.0	2.6
37	19.0	35.0	4.0
38	18.3	50.0	4.9

Note.—Cases 35 and 36 are the same patient.

No patient had been operated on or had received chemotherapy, radiation therapy, or steroid medication which might change the blood-brain barrier. At least 24 hr elapsed between the patient's enhanced CT scan and the dual kilovoltage study.

Mathematical Determinations

The mathematical derivations of the effective atomic number and electron density of a material have been determined by several investigators [2-4], and the techniques for finding these values for intracranial tumors has been reported [1]. Briefly, a probable intracranial neoplasm was identified on an enhanced CT scan. After an interval of at least 24 hr, a representative area of the tumor as seen on the original study was rescanned before the administration of contrast at two different kilovoltage settings. Contrast material was administered and scans made at the same level, again with the two kilovoltage settings, so that a total of four scans was performed. All scanning was done on a Pfizer 0100 scanner, using 90 and 130 kVp.

The average linear attenuation coefficient, μ, of a 9 × 9 mm (36 pixels) area of the neoplasm was determined on each scan. Only areas of enhancement within the tumor were evaluated, with a portion selected that appeared to be homogeneous in its enhancement. Once an area on the enhanced scan was selected, the same area was found by its coordinates on the unenhanced scan and evaluated. Frequently, multiple areas were evaluated and averaged to insure that a representative portion of the tumor was sampled. Only an area of enhancement in tumors with a "ring sign" was evaluated; care was taken to avoid partial volume errors by including low density regions within the ring.

Because the Pfizer 0100 scanner is not calibrated against a standard material during each translation, its number scale is expressed in relative rather than absolute terms. As explained previously [1], we have used normal brain as a standard for determining the linear attenuation coefficients within the tumor. We selected an area of normal brain in the opposite hemisphere in a position symmetrical to the neoplasm to use as this internal standard.

The effective atomic number, Z, before contrast was determined by applying the ratio of the coefficients at the two energy levels to a graph which relates the attenuation coefficient ratio to the effective atomic number [1]. The process was repeated for values following contrast enhancement. The percentage change of Z after enhancement relative to the precontrast values is expressed as:

$$\% \Delta Z = \frac{Z_{contrast} - Z_{no\ contrast}}{Z_{no\ contrast}} \times 100$$

The linear coefficients, used to calculate the effective atomic number, can themselves be evaluated. The "μ-shift" of the tumor is defined as the percentage change of the average linear attenuation coefficient at one kilovoltage setting after enhancement relative to the precontrast value, shown as follows for 90 kVp:

$$\% \Delta \mu_{90} = \frac{\mu_{90} (contrast) - \mu_{90} (no\ contrast)}{\mu_{90} (no\ contrast)} \times 100$$

The "μ-shift" at 130 kVp is determined in similar fashion. The "μ-spread" represents the change of precontrast linear attenuation coefficients with enhancement and also takes into account the change of kilovoltage. It is expressed as:

$$\mu\text{-spread} = \frac{(\mu_{90} - \mu_{130})_{contrast} - (\mu_{90} - \mu_{130})_{no\ contrast}}{(\mu_{90} - \mu_{130})_{no\ contrast}}$$

Analysis of variance was used to compare mean CT scan measurements among different histologic categories.

Accuracy of the Method

The Pfizer 0100 scanner has an exposure time of 4.5 min, long by today's standards. Because the study began in 1976 and ex-

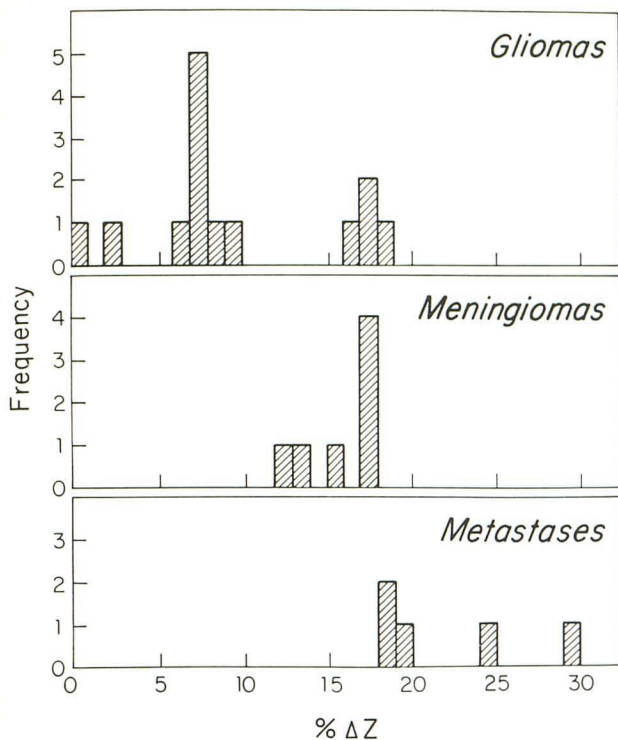


Fig. 1.—Preoperative prediction of histology based on frequency distribution of %ΔZ.

tended through 1978, consistency of equipment variables required the continued use of the same scanner. With such a long exposure time, patient motion might have introduced significant inaccuracy. However, motion was held to a minimum with sedation, and the scans obtained were surprisingly free of motion artifact; cases were discarded if there was significant motion.

An area of 36 pixels was used to determine the mean linear attenuation coefficient within the tissue evaluated. Initially, sample areas up to 100 pixels were used, but the results did not differ significantly from those using 36 pixels, and the mathematics were easier with the smaller volume. Others [5] have indicated that the standard deviation about a mean value (noise) is relatively independent of sample size if 25 or more pixels are used in the sampling.

We verified the effective atomic number by scanning a series of pins of different composition within a water phantom and comparing our results to published values. As indicated earlier [1], our method is accurate to about 3%, similar to accuracies reported by others [2]. We have determined experimentally that beam-hardening effects by fortuitous position of the tumor within the skull may amount to 3%. Such an error should not be a consideration here, however, since the symmetrical area of normal brain in the opposite hemisphere, used as an internal standard, would be subjected to the same beam hardening and therefore cancel the effect on the tumor values.

Results

The values of %ΔZ, μ-spread, and μ-shift at 90 kVp are listed for each of the 38 tumors in table 1. To test these values in the preoperative prediction of histology, the 26 cases of gliomas, meningiomas, and metastases have been

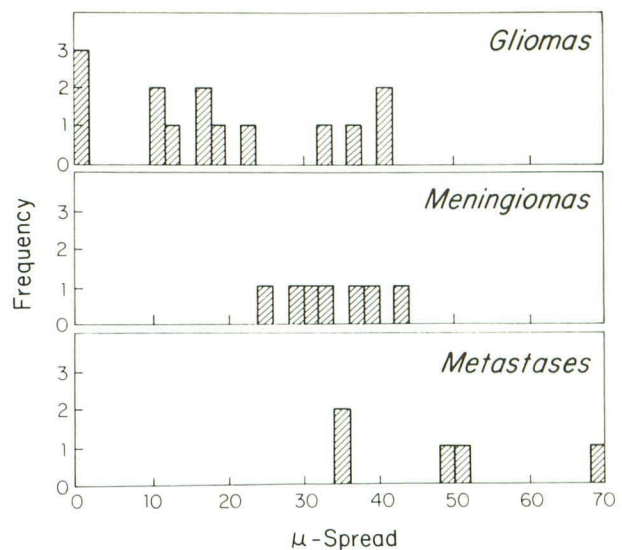


Fig. 2.—Preoperative prediction of histology based on frequency distribution of μ spread.

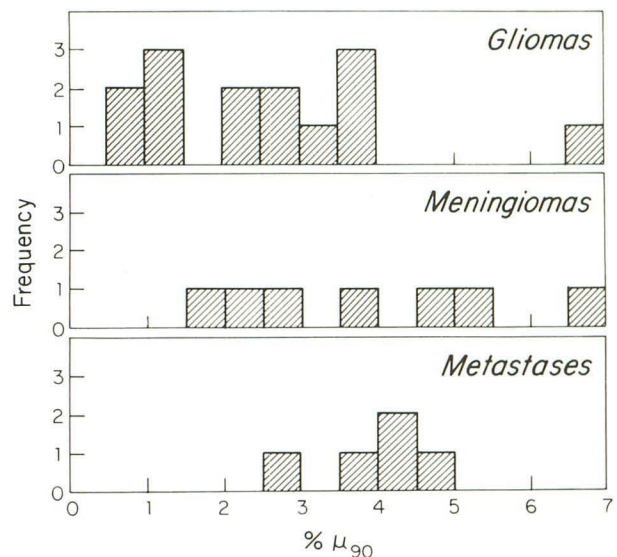


Fig. 3.—Preoperative prediction of histology based on frequency distribution of %μ90.

graphed in frequency distributions as a function of %ΔZ (fig. 1), μ-spread (fig. 2), and μ-shift-90 (fig. 3).

It is evident from figure 1 that %ΔZ produces excellent separation of the three classes of neoplasms with four exceptions. Case 4 was an aggressive glioma in a child; case 14 was an extremely vascular and aggressive medulloblastoma in a child; case 11 was a large exophytic brainstem astrocytoma in an adult; and case 10 was a tumor whose histology was difficult to interpret. The last was so anaplastic that differentiation between a metastasis and a glioblastoma was difficult, with the latter diagnosis favored. The childhood tumors acted in a malignant fashion, with early death, as did the fourth case with the problematic histology. If these four cases are excluded, the three groups

are totally separated using $\% \Delta Z$. The differences among means of the three groups, even with the four cases included, are statistically significant with $p < 0.0005$.

Figure 2 shows the predictive value of the μ -spread function. There is no overlap between the gliomas and meningiomas if the four cases mentioned are excluded; however, meningiomas and metastases do overlap. While there is a close correlation between $\% \Delta Z$ and μ -spread ($r = 0.96$), as might be expected from the similarity of the terms in the equations, the differences among means for μ -spread are slightly less significant ($p < 0.001$) and the overlap of groups is apparent.

Figure 3 demonstrates the frequency distributions using $\% \Delta \mu$ at 90 kVp. There is much overlap of tumor classes, and no statistically significant separation. Previous work [1] showed even less separation using $\% \Delta \mu$ at 130 kVp.

The 14 cases of gliomas were evaluated separately, correlating predominant histologic grade with $\% \Delta Z$. As shown in figure 4, there is overlap of the $\% \Delta Z$ values, so that while $\% \Delta Z$ is effective in predicting the presence of a glioma, it is not useful in predicting its histologic grade.

The $\% \Delta Z$ values for the remaining 12 cases proved helpful in most instances. All acoustic neurinomas had values above the meningioma range, extending into the values of the metastatic tumors. Since the radiographic appearances were not those of metastases, the values would help in differentiating between the two common cerebellopontine angle masses, acoustic neurinoma and meningioma. Two of the three histiocytic lymphomas had values in the meningioma range. The intraparenchymal location of the tumors excluded meningioma, but the $\% \Delta Z$ values suggested a lesion other than the typical gliomas or metastasis. Therefore, while a characteristic $\% \Delta Z$ value was not found for each tumor type, the values did aid in the differential diagnosis, given the appropriate radiographic presentation.

Three cases illustrate the help in differential diagnosis. Figure 5 (case 9) demonstrates a left temporal mass with slightly increased density before contrast and a homogeneous degree of enhancement of a well demarcated tumor. The lack of more dramatic mass effect considering the size of the lesion suggested its slow growth. Angiography showed a diffuse and persisting blush, and the radiographic diagnosis was a meningioma. However, the determinations of $\% \Delta Z$ and μ -spread suggested another diagnosis. Z without contrast was 7.1, Z with contrast was 7.6, and $\% \Delta Z$ was 7.0; μ -spread was 16.6. These values were in the glioma range, not the meningioma group. At surgery, a well circumscribed glioma was found which was infiltrating into the insular parenchyma. Histologically, this was a grade 4 astrocytoma (glioblastoma).

Figure 6 (case 8) demonstrates two ringlike lesions with abundant cerebral edema in the left frontal lobe. Two contiguous metastases were considered, although no other intracranial lesions were found. However, the $\% \Delta Z$ value of 7.0 and the μ -spread value of 11.7 were in the glioma category, not the metastatic group. At surgery, a horseshoe-shaped glioblastoma was found. In figure 7 (case 31), a poorly margined neoplasm of the superior cerebellum is shown in a 75-year-old man. While not as circumscribed as

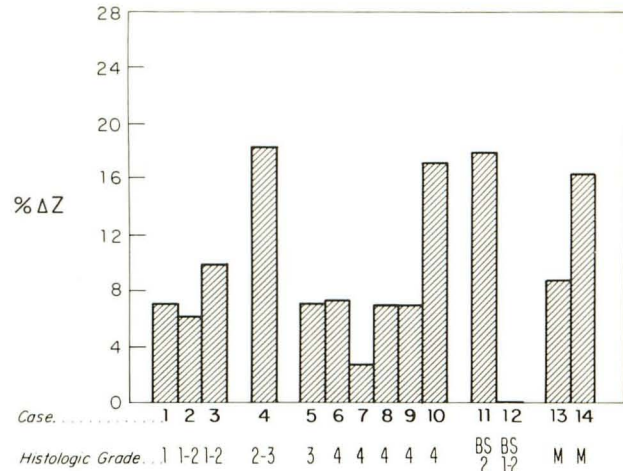


Fig. 4.—Evaluation of 14 cases of glial tumors. Predominant histologic features were correlated with $\% \Delta Z$. BS = brainstem. M = medulloblastoma.

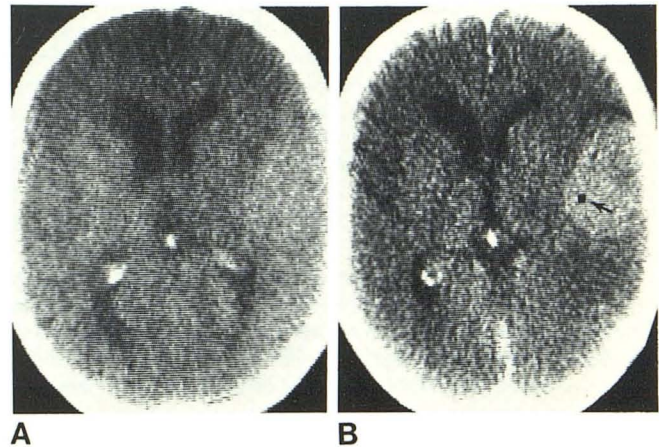


Fig. 5.—Case 9. A, Large left temporal lobe mass is slightly dense on nonenhanced CT scan. B, Scan with contrast material shows sharp borders and homogeneous enhancement. Square (arrow) denotes area sampled to determine μ and Z. Left carotid angiography (not shown) demonstrated diffuse tumor blush that persisted through venous phase. Preoperative diagnosis was meningioma.

most hematogeneous metastases, primary gliomas of the cerebellum are not common in this age group. Nevertheless, these were the two primary radiographic diagnoses. The $\% \Delta Z$ value of 15.0, however, was not in either the glioma or metastasis group, suggesting another diagnosis. The μ -spread value of 34.0 was less helpful, since there was overlap of the glioma and metastasis groups in the 30–40 range. At surgery, a histiocytic lymphoma was found. One other histiocytic lymphoma had a similar $\% \Delta Z$ value, while a third case had a value in the metastatic range.

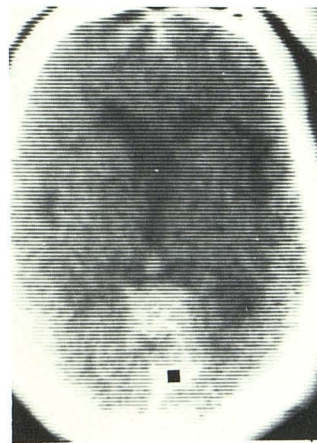
Discussion

The determination of the change of effective atomic number with contrast enhancement is a sensitive technique for

Fig. 6.—Case 8. Enhanced scan shows two apparently separate cystic or necrotic masses in left frontal lobe. Differential diagnosis included two metastases and irregularly shaped glioma. Square (arrow) is sampled area.



Fig. 7.—Case 31, 75 year-old-man. Enhanced CT scan shows poorly margined enhancing mass in superior aspect of cerebellum. There is mild hydrocephalus. Square is sampled area.



measuring the amount of iodinated contrast material that passes into and is retained by an intracranial neoplasm. Contrast material crosses an abnormal blood-brain barrier if the lesion is within the parenchyma. Extraparenchymal lesions outside the normal blood-brain barrier also collect contrast material, presumably within vascular structures such as sinusoids or by passing a blood-tissue interface to collect in the interstices of the neoplasm. Increasing the effective atomic number of a material, particularly with a high atomic numbered substance such as iodine, allows for a greater degree of photoelectric absorption of incoming x-rays. This makes the dual kilovoltage technique, with its relatively low kilovoltage settings of 90 and 130 kVp, a sensitive method for measuring the amount of retained contrast material in the neoplasm.

At first, it may be thought that $\% \Delta Z$ is a measurement of the degree of breakdown of the blood-brain barrier, with more malignant lesions having a larger $\% \Delta Z$ than less malignant ones. For example, metastatic tumors would have a greater percentage change than low grade gliomas. Authors [6] have suggested that the grade of a glioma could be predicted by the degree of enhancement, with the low grade gliomas showing little enhancement and the high grade gliomas enhancing to a marked degree.

This seems too simplistic, however. First, most benign extraparenchymal neoplasms outside the blood-brain bar-

rier retain a greater amount of contrast per unit volume than most gliomas, benign or malignant. This enhancement is not dependent on vascularity, in which case the contrast would wash out relatively soon, but represents retention in the sinusoids or interstices of the tumor. Second, gliomas may be grossly malignant histologically, yet not have nearly the degree of enhancement as parenchymal metastases. In addition, the degree of contrast enhancement of gliomas is not proportional to the grade of the glioma. While the pathologic grading of a tumor depends on the material submitted for histologic review, and therefore may not reflect the entire tumor, the series of 14 gliomas in our study certainly shows a lack of correlation between the degree of enhancement ($\% \Delta Z$) and histologic grade. Finally, previous work [7] has shown a lack of enhancement in medium to high grade gliomas and metastases, many are of low density due to microcystic change. Thus, the lack of enhancement of a neoplasm does not preclude its malignancy.

Our results indicate that the change in effective atomic number with contrast enhancement correlates closely with brain tumor histology. Other measurements vary from markedly to slightly less accurate. Measurements of the linear attenuation coefficients themselves, and their change with contrast enhancement, at only one kilovoltage do not have the sensitivity in evaluating the amount of high atomic numbered materials such as iodine inherent in the dual kilovoltage technique. Histology cannot be predicted using the linear attenuation coefficients at only one kilovoltage setting. The basic CT numbers are proportional to the linear attenuation coefficients. Previous work with these numbers and various statistical manipulations of them has shown the lack of accuracy of these values, whether before or after contrast, in predicting histology [1]. The " μ -spread" method is similar to that used to find $\% \Delta Z$, since it uses not only pre- and postcontrast values but also the changing kilovoltage. The results are slightly less accurate, and there is some overlap of values not present in the $\% \Delta Z$ method. The mathematical differences in the two methods and the reasons for the lesser accuracy have been discussed [1].

We emphasize that evaluations of this type can be performed on any CT unit. The mathematics described were developed for a whole body unit which does not scan a standard material with every pass. The majority of CT units available today fit this description and only minor mathematical alterations would be necessary for a scanner that standardizes during each run. The accuracy of our method may suffer from patient motion due to the long scanning time, and it will be interesting to evaluate the results on the rapid high resolution systems that will allow precise measurements.

REFERENCES

1. Latchaw RE, Payne JT, Gold LHA. Effective atomic number and electron density as measured with a computed tomography scanner: computation and correlation with brain tumor histology. *J Comput Assist Tomogr* 1978;2:199-208
2. Rutherford RA, Pullan BR, Isherwood I. Measurement of effective atomic number and electron density using an EMI scanner. *Neuroradiology* 1976;11:15-21

3. McDavid WD, Waggener RG, Dennis MJ, Sank UJ, Payne WH. Estimation of chemical composition and density from computed tomography carried out at a number of energies. *Invest Radiol* **1977**;12:189-194
4. McCullough EC. Photon attenuation in computed tomography. *Med Phys* **1975**;2:307-320
5. McCullough EC, Payne JT, Baker HL, et al. Performance evaluation and quality assurance of computed tomography scanners, with illustrations from the EMI, ACTA, and Delta scanners. *Radiology* **1976**;120:173-188
6. Hilal SK, Chang CH. Value of CT as an index of malignancy of brain tumors. Presented at the annual meeting of the American Society of Neuroradiology, New Orleans, February **1978**
7. Latchaw RE, Gold LHA, Moore JS, Payne JT. The nonspecificity of absorption coefficients in the differentiation of solid tumors and cystic lesions. *Radiology* **1977**;125:141-144